Development 140, 916-925 (2013) doi:10.1242/dev.091066

Genetic lineage labeling in zebrafish uncovers novel neural crest contributions to the head, including gill pillar cells

Alessandro Mongera[1,*], Ajeet P. Singh[1], Mitchell P. Levesque[1,‡], Yi-Yen Chen[1,§], Peter Konstantinidis[2] and Christiane Nüsslein-Volhard[1,*]

SUMMARY

At the protochordate-vertebrate transition, a new predatory lifestyle and increased body size coincided with the appearance of a true head. Characteristic innovations of this head are a skull protecting and accommodating a centralized nervous system, a jaw for prey capture and gills as respiratory organs. The neural crest (NC) is a major ontogenetic source for the 'new head' of vertebrates and its contribution to the cranial skeleton has been intensively studied in different model organisms. However, the role of NC in the expansion of the respiratory surface of the gills has been neglected. Here, we use genetic lineage labeling to address the contribution of NC to specific head structures, in particular to the gills of adult zebrafish. We generated a *sox10:ER^{T2}-Cre* line and labeled NC cells by inducing Cre/loxP recombination with tamoxifen at embryonic stages. In juvenile and adult fish, we identified numerous established NC derivatives and, in the cranium, we precisely defined the crest/mesoderm interface of the skull roof. We show the NC origin of the opercular bones and of multiple cell types contributing to the barbels, chemosensory organs located in the mouth region. In the gills, we observed labeled primary and secondary lamellae. Clonal analysis reveals that pillar cells, a craniate innovation that mechanically supports the filaments and forms gill-specific capillaries, have a NC origin. Our data point to a crucial role for the NC in enabling more efficient gas exchange, thus uncovering a novel, direct involvement of this embryonic tissue in the evolution of respiratory systems at the protochordate-vertebrate transition.

KEY WORDS: Neural crest, Pillar cells, Cre/loxP, Zebrafish, Cranial neural crest, Gill

INTRODUCTION

The evolution of a true head has been proposed as a major step in the protochordate-vertebrate transition, enabling the shift from filter feeding to active predation (Northcutt and Gans, 1983). The vertebrate head that has been assembled stepwise over evolutionary time displays functional characteristics that serve prey detection and capture but also enable a more efficient respiratory metabolism (Gans and Northcutt, 1983). Indeed, a predatory lifestyle requires a higher metabolic rate, which in turn establishes a positive selective pressure for enhanced gas exchange and distribution. To increase gas exchange capacity, respiration shifted during evolution from ciliated epithelia along the walls of the pharynx to complex gill organs attached to the branchial arches. Craniates, which include vertebrates and hagfishes, developed gills with highly organized filamentous structures that enable a massive expansion of the surface area involved in respiration (Evans et al., 2005).

The 'new head' theory of Northcutt and Gans proposes that many morphological and functional innovations of vertebrates develop from the neural crest (NC), the epidermal placodes or the lateral plate mesoderm (Northcutt and Gans, 1983). Although the original claims of this theory regarding the origin of NC and placodes have been subsequently refuted, a huge body of work has confirmed the important role of NC in accelerating vertebrate evolution (Northcutt, 2005; Yu et al., 2008; Abitua et al., 2012). NC is a pluripotent embryonic tissue that differentiates into numerous cell types, such as osteoblasts and chondroblasts in the skull, neurons of the peripheral nervous system, Schwann cells and pigment cells (Hörstadius, 1950; Le Douarin, 1986; Le Douarin and Dupin, 2012). Further, NC is suggested to have played a crucial role in vertebrate brain development by promoting forebrain viability, a prerequisite for brain expansion (Etchevers et al., 1999).

Although the NC origin of the cartilaginous gill arch endoskeleton (Landacre, 1921) and of the walls of pharyngeal blood vessels (Le Lièvre and Le Douarin, 1975) is long established, the embryonic origin of gill pillar cells, which represent the functional and structural core of the gill lamellae, is unclear (Hughes and Morgan, 1973). It has been suggested that this important component of the gill filaments might derive from the lateral plate mesoderm (Northcutt and Gans, 1983), from endothelial cells (Bietrix, 1895) or from smooth muscles (Datta Munshi and Singh, 1968).

Extensive fate mapping of NC has been performed in many organisms representative of different vertebrate taxa (Le Douarin and Kalcheim, 1999), notably by transplantation experiments creating chick-quail chimeras (Le Douarin, 1986), vital dye injection in the premigratory NC of chick and frog (Bronner-Fraser and Fraser, 1988; Collazo et al., 1993), tissue extirpation in medaka and lampreys (Langille and Hall, 1988a; Langille and Hall, 1988b), and genetic lineage labeling using Cre/loxP-mediated recombination in mice (Chai et al., 2000; Jiang et al., 2002). However, a more detailed map for adult structures in hagfishes, lampreys and ray-finned fishes (actinopterygians) would be extremely valuable, as important structures of the 'new head', such as the gills, were lost very early in the evolution of tetrapods with the acquisition of a terrestrial lifestyle. In zebrafish and medaka, vital dye injection, expression of reporter genes and transplantation experiments have been employed to follow the migration of NC-

[1]Max-Planck-Institut für Entwicklungsbiologie, 72076 Tübingen, Germany. [2]Institut für Spezielle Zoologie und Evolutionsbiologie mit Phyletischem Museum, Friedrich-Schiller-Universität Jena, 07743 Jena, Germany.

*Authors for correspondence (alessandro.mongera@tuebingen.mpg.de; christiane.nuesslein-volhard@tuebingen.mpg.de)
‡Present address: University of Zurich Hospital, 8091 Zurich, Switzerland
§Present address: GeneTex International Corporation, 300 Hsinchu, Taiwan

Accepted 12 December 2012

derived cells in the larva (Langille and Hall, 1988a; Schilling and Kimmel, 1994; Li et al., 2003; Wada et al., 2005). However, these methods have severe limitations as far as adult structures are concerned, as the label becomes diluted or transgene expression does not persist through adulthood.

To overcome these limitations and to permanently and specifically label NC cells and their derivatives in zebrafish, we generated a transgenic line expressing tamoxifen-inducible Cre recombinase under the control of the *sox10* promoter (Carney et al., 2006). *Sox10* is expressed specifically in the NC at early stages of development (Dutton et al., 2001). We induced Cre/loxP-mediated recombination in various reporter lines during embryonic development and identified in larval, juvenile and adult fish numerous established NC derivatives, including multiple elements of the cranial skeleton, peripheral nervous system components, pigment cells and glia, thus confirming the specific expression of the *sox10* promoter in NC cells during the time of induction.

Moreover, we were able to define the NC/mesoderm interface in the zebrafish frontoparietal bones, which are dermoskeletal elements whose origin across vertebrate taxa is still debated (Couly et al., 1993; Gross and Hanken, 2008a; Noden and Trainor, 2005), and to demonstrate a NC contribution to other head structures of uncertain origin.

Strikingly, we observed labeled gill filaments, including primary and secondary lamellae. In particular, we discovered labeled pillar cells, which represent a craniate innovation that provides the basis for the surface expansion of the gills (Evans et al., 2005). Pillar cells form capillary beds for blood perfusion and have mechanosensory properties (Smith and Chamley-Campbell, 1981; Evans et al., 2005). We propose that the development of this atypical NC-derived cell type at the protochordate-vertebrate transition led to the appearance of a more complex gill organ, supporting the relevance of the 'new head' theory to the evolution of the respiratory system.

MATERIALS AND METHODS

Transgenic lines

To generate *Tg(cmlc:GFP-sox10:ER^{T2}-Cre)* (abbreviated to *sox10:ER^{T2}-Cre*), the *(−4.9kb)sox10* promoter (Carney et al., 2006) was subcloned into a pTol2-*cmlc:GFP* plasmid and the ER^{T2}-Cre coding sequence (Metzger et al., 1995) was PCR amplified and inserted by in-fusion reaction (Clontech) downstream of the promoter region. For *Tg(rps9:loxP-DsRed2-loxP-EGFP)* (abbreviated to *rps9:switch*), the *EF1α* promoter in the pTol-*EF1α*:loxP-DsRed2-loxP-EGFP plasmid (Hans et al., 2009) was replaced with a 3 kb promoter region of the Fugu *rps9* gene (ENSTRUG00000015896.1). Primers used: 5′-AGAATCAC-CGTGGGTGAGGAG-3′ and 5′-GGCGGCTTAATTGTGCCTGCA-3′. In addition, the following reporter lines were used: *Tg(β-actin2:loxP-STOP-loxP-DsRed-express)* (abbreviated to *β-actin:switch*) (Bertrand et al., 2010); *Tg(ubi:loxP-EGFP-loxP-mCherry)* (abbreviated to *ubi:switch*) (Mosimann et al., 2011); *Tg(EF1α*:loxP-DsRed2-loxP-EGFP) (abbreviated to *EF1α:switch*) (Hans et al., 2009); *Tg(hsp70l:loxP-DsRed2-loxP-nlsEGFP)* (abbreviated to *hs:R to nG*) (Knopf et al., 2011); *Tg(crestin:Gal4-UAS-GFP)* (Y.-Y. Chen, PhD thesis, Eberhard Karls Universität Tübingen, 2011); and *Tg(−4725sox10:Cre)* (Rodrigues et al., 2012).

For early NC tracing (within the first 3 days), the best line is *EF1α:switch*, as the expression level is high at early stages. For metamorphic and adult fish, the best 'ubiquitous' line in our experience is *ubi:switch*, followed by *β-actin:switch*, which generally leads to a more patchy labeling.

Cre induction

Fish carrying the *sox10:ER^{T2}-Cre* transgene were crossed to the different reporter lines and 16-hpf embryos were dechorionated and treated with 5 μM 4-hydroxytamoxifen (4-OHT; Sigma, H7904) for 8 hours unless otherwise specified. Control embryos were incubated in a corresponding dilution of ethanol.

UAS:Cre injection

Tg(crestin:Gal4-UAS-GFP;β-actin:switch) embryos at the 1-cell stage were injected with different concentrations (1-10 ng/μl) of a pTol2 vector containing the Cre coding sequence downstream of a 4xUAS site.

Image acquisition and processing

Images were taken using a Zeiss LSM 5 Live confocal microscope and a Leica M205 FA stereomicroscope and processed using Imaris (Bitplane), ImageJ (NIH) and Adobe Photoshop. For confocal imaging of adult gills, fish were fixed for 1 hour in 4% paraformaldehyde. The head was mounted in 0.4% agarose for imaging after the removal of the operculum. Adult maxillary barbels were surgically removed and mounted in 1% agarose for imaging.

Cryosectioning and immunohistochemistry

After fixation, juvenile fish (1 mm) were washed with PBS and incubated in 10%, 20% and 30% sucrose solutions. The samples were then incubated in 1:1 30% sucrose:OCT Compound (Tissue-Tek) for 30 minutes and then in OCT overnight. Fish were frozen in cryomolds and 20 μm cryosections were obtained with a CH3050 cryostat (Leica). Cryosections were treated with 100% methanol for 10 minutes to improve adherence to the slides. Sections were rehydrated in PBST (PBS with 0.1% Tween 20), and blocked in 10% sheep serum in PBST for at least 1 hour at room temperature. The primary antibody [rabbit anti-DsRed (Clontech) at 1:200] was incubated overnight at 4°C in 10% sheep serum in PBST. Sections were then washed with PBST and incubated with the secondary antibody [anti-rabbit-Cy3 (Dianova) at 1:400] for 2 hours at room temperature. Sections were washed several times with PBST and nuclei visualized by adding DAPI (Sigma) to PBST in the last washing step.

RESULTS

sox10:ER^{T2}-Cre allows inducible labeling of NC in zebrafish

We generated a *sox10:ER^{T2}-Cre* transgenic line by fusing the NC-specific *(−4.9kb)sox10* promoter to the tamoxifen-inducible Cre recombinase coding sequence [Fig. 1A (1)]. To test the system prior to NC differentiation, we created a reporter line that ubiquitously drives a red-to-green switchable cassette under the control of the Fugu *(−3)rps9* promoter [Fig. 1A, before (2) and after (3) recombination]. The recombination was induced in double-transgenic embryos carrying the Cre driver construct and the reporter cassette by adding 4-hydroxytamoxifen to the water for 8 hours [16-24 hours postfertilization (hpf)], when NC delamination and early migration occur (Fig. 1B). At this time period, the *sox10* promoter is reported to be specific for NC cells and oligodendrocytes (Simon et al., 2012; Carney et al., 2006). To assess the controllability and the potential leakiness of the system, we compared induced and uninduced embryos at 36 hpf. After induction we found many GFP$^+$ cells resulting from Cre-induced recombination in the branchial arch region (Fig. 1C), in the dorsal neural tube, around the otic vesicles (Fig. 1E) and along the walls of the dorsal aorta and the ventral notochord (Fig. 1G). Uninduced embryos lacked GFP$^+$ cells in these areas (Fig. 1D,F,H).

We then induced clones in the well-established *β-actin:switch* reporter line, which has already been shown to effectively trace embryonic cell populations to later stages of development and to adulthood (Bertrand et al., 2010). We analyzed the developing viscerocranium in larvae at 4 days postfertilization (dpf). In this

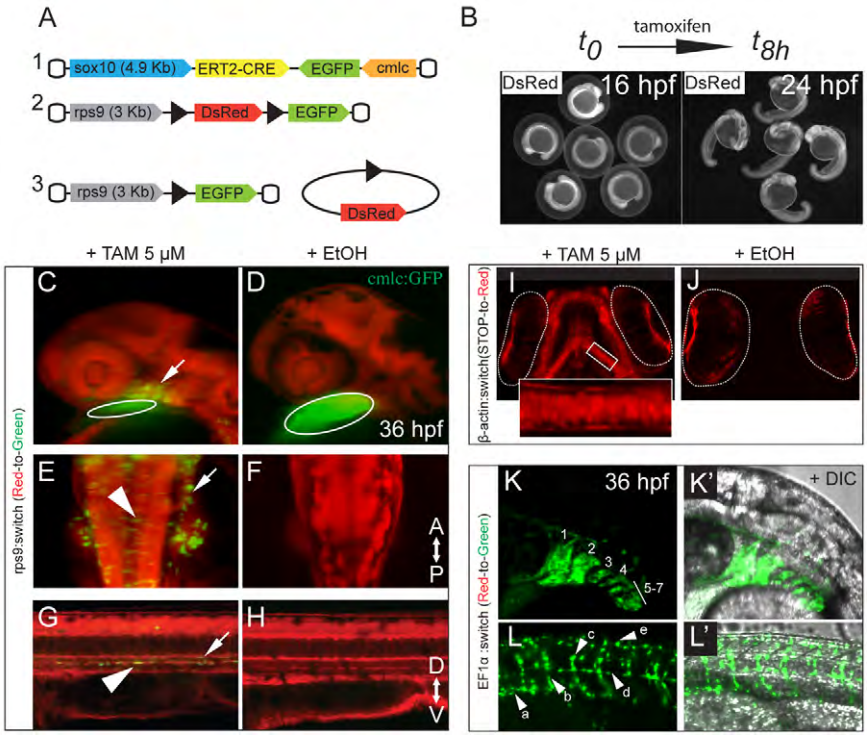

Fig. 1. An inducible Cre/loxP-based genetic system for long-term fate mapping of zebrafish NC. (**A**) Schematic of the two constructs used to generate (1) a NC-specific *ER^{T2}-Cre* driver line [*(–4.9kb)sox10* zebrafish promoter] and (2) a ubiquitous reporter line [*(–3kb)rps9* promoter from *Takifugu rubripes*] that enables detection of the recombination events during the early phases of NC differentiation. (3) *DsRed* excision after Cre-mediated recombination. (**B**) Time window for tamoxifen induction (16-24 hpf). (C-H) *Tg(sox10:ER^{T2}-Cre;rps9:switch)* embryos at 36 hpf, treated with tamoxifen (C,E,G) or with ethanol as control (D,F,H). (C-L′) Maximum intensity projections (MIPs) of confocal stacks. (**C**) GFP$^+$ recombined cells in the branchial arch region (arrow) and cmlc:GFP marker (circled). (**E**) Hindbrain area with recombined cells in the otic epithelium (arrow) and along the dorsal neural tube, characterized by an epithelial, pre-delamination shape (arrowhead). (**G**) Sagittal section of the trunk with GFP$^+$ melanoblasts and sympathetic neuron precursors flattened along the dorsal aorta walls (arrowhead) and the ventral notochord (arrow). (**D**,**F**,**H**) In the uninduced controls, no recombined cells are detectable. (**I**,**J**) Developing viscerocranium in 4-dpf *Tg(sox10:ER^{T2}-Cre;β-actin:switch)* larvae showing labeled chondrocytes that are absent in the control. The eyes, which show red autofluorescence, are circled. (**K-L′**) *Tg(sox10:ER^{T2}-Cre;EF1α:switch)* induced embryos (36 hpf) showing (K,K′) labeled pharyngeal arches (1-7) and (L,L′) pigment precursors (a), motor axon glia (b), dorsal root ganglia (DRG) progenitors (c), glia along the lateral line (d) and dorsal melanoblasts (e). The anteroposterior (AP) and dorsoventral (DV) axes are indicated.

region, chondroblasts were labeled in induced larvae (n=10; Fig. 1I), whereas no DsRed$^+$ cells were detected in uninduced controls (n=10; Fig. 1J). Next, we analyzed the specificity of our system for NC derivatives using the *EF1α:switch* line and observed specific marking of pharyngeal arches 1-7 (Fig. 1K,K′) and of pigment precursors, peripheral nervous system glia, dorsal root ganglia (DRG) progenitors, lateral line Schwann cells and dorsal melanoblasts (Fig. 1L,L′, a-e, respectively). Induction of Cre at later time points (4 dpf) and for shorter periods (1-2 hours) results in isolated clones restricted to one or a few cell types, such as pigment cells (supplementary material Fig. S1A,D; n=50). These clones become smaller when the induction is performed at juvenile stages (i.e. 20 dpf; n=46; supplementary material Fig. S1B). Lack of labeling in adults of uninduced fish carrying both transgenes (supplementary material Fig. S1C) suggests that reporter expression was under tight control of the externally supplied tamoxifen.

Taken together, these results show that the *sox10:ER^{T2}-Cre* line allows for rigorous control of the onset of tamoxifen-dependent recombination events in NC cells. In line with the previously characterized *(−4.9)sox10:GFP* reporter (Carney et al., 2006), our *sox10:ER^{T2}-Cre* is occasionally expressed in a few random skeletal muscle progenitors in the trunk, which appear through adulthood as labeled clones (data not shown). These rare clones (on average one per flank), along with their clonally related recombined tissues, were not considered further in this analysis.

NC-derived structures in the trunk

To assess the NC contribution to postembryonic structures, we first analyzed labeled tissues in established postcranial NC derivatives of metamorphic juvenile fish (20 dpf) in which recombination had been induced at embryonic stages as described above (Fig. 2). We detected sympathetic ganglia (Fig. 2A), neurons of the enteric nervous system (Fig. 2B) and DRG (Fig. 2C). Moreover, we found sensory neurons innervating the body periphery, such as the pectoral and the caudal fins (Fig. 2D,D′, respectively). Glia providing myelination to axons in the peripheral nervous system were also marked (Fig. 2E-F′). We then searched for labeled chromatophores and found clones of iridophores, melanophores and xanthophores (Fig. 2G-I′). In several cases, we found labeled melanophores in proximity to recombined glial cells that surround the DRG (Fig. 2J, arrowheads).

In the heart of metamorphic switched fish we found many labeled cells, of which at least some show overlap with *cmlc:GFP*$^+$ cells, indicating that they are contractile cardiomyocytes (Kwan et al., 2007) (Fig. 2K,K′). In zebrafish, by means of cell

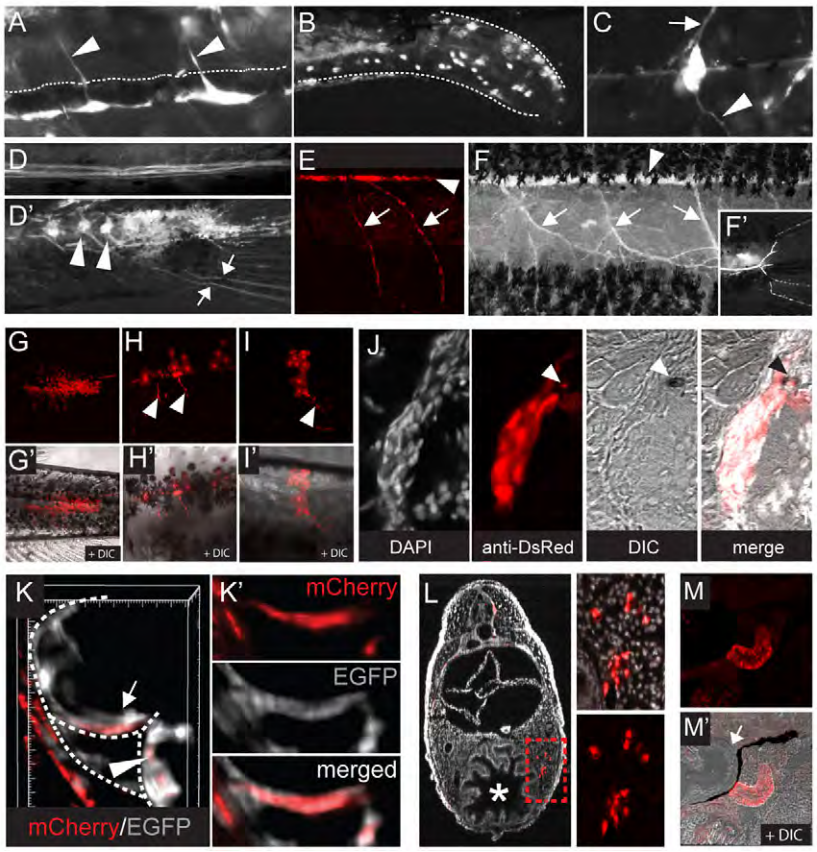

Fig. 2. Detection of postcranial NC derivatives. (**A-D′**) Lateral perspectives of epifluorescent acquisitions of DsRed$^+$ components of the peripheral nervous system in induced *Tg(sox10:ER^{T2}-Cre;β-actin:switch)* metamorphic fish. (A) Sympathetic ganglia (white) located along the ventral walls of the dorsal aorta (the dorsal walls are highlighted by the dashed line) and axonal projections (arrowheads) towards the spinal chord. (B) Neurons located in the most posterior region of the gut (dashed lines), close to the anus, forming the enteric nervous system. (C) DRG with afferent (arrow) and efferent (arrowhead) projections. (D,D′) Somatosensory projections innervating the pectoral fin (D) and the caudal fin (D); indicated are two of the most posterior DRG in the caudal region (arrowheads) and their projections entering the fin region (arrows). (**E-F′**) DsRed$^+$ glia cells in induced *Tg(sox10:ER^{T2}-Cre;β-actin:switch)* metamorphic and adult fish. MIP of confocal stacks showing glia cells along the lateral line nerve (arrowhead) and the axonal projections innervating the neuromasts (arrows) in metamorphic (E) and adult (F) zebrafish. (F′) Lateral line glia in the caudal fin. (F,F′) Epifluorescence pictures. (**G-I′**) MIP of confocal stacks showing pigment cells in induced *Tg(sox10:ER^{T2}-Cre;β-actin:switch)* metamorphic fish: (G,G′) iridophore clone, (H,H′) melanophore clone with glia cells (arrowheads) and (I,I′) xanthophore clone with glia cells (arrowhead). (**J**) Confocal image of transverse cryosection and anti-DsRed antibody staining showing a labeled melanophore (arrow) close to labeled glia cells wrapped around the DRG. (**K**,**K′**) Heart region of induced metamorphic fish carrying the *ubi:switch* transgene as a reporter. (K) 3D view of confocal stacks showing cmlc:GFP$^+$ cardiomyocytes (gray) and mCherry$^+$ cells (red, arrow and arrowhead) in the heart. (K′) Confocal section of the region indicated in K by the arrow, showing colocalization between an mCherry$^+$ cell and a GFP$^+$ cardiomyocyte. (**L**) Confocal image of transverse cryosection and anti-DsRed antibody staining showing an induced *Tg(sox10:ER^{T2}-Cre;β-actin:switch)* metamorphic fish. Labeled adrenomedullary cells in the liver (red, inset). The gut is indicated by the asterisk. (**M**,**M′**) Confocal image of sagittal cryosection and anti-mCherry antibody staining showing the pronephric duct region of an induced *Tg(sox10:ER^{T2}-Cre;ubi:switch)* metamorphic fish. (M) mCherry$^+$ cells populate the epithelial walls of the pronephric duct. (M′) The arrow indicates the otic capsule in the posterior chondrocranium.

transplantation and different labeling techniques, a NC contribution to cardiomyocytes has already been demonstrated (Sato and Yost, 2003; Li et al., 2003). We also observed clones in the adrenomedullar region (Fig. 2L) and in the epithelial walls of the pronephros (Fig. 2M,M′), confirming the NC contribution to these internal organs (Collazo et al., 1993).

Taken together, these data show that our inducible Cre/loxP-based genetic labeling system enables the detection of a large set of trunk NC derivatives in juvenile and adult fish. With the rare exception of spurious muscle clones, we did not detect any tissue with an established non-NC origin. The *sox10:ER^{T2}-Cre*-induced recombination may thus be used as a potent tool to uncover the NC origin of other postembryonic structures.

Analysis of labeled head structures reveals a NC contribution to frontal but not parietal bones

Next, we surveyed labeled chondrocranial and cartilaginous viscerocranial elements of the developing skull in 5-dpf larvae (Schilling et al., 1996; Piotrowski et al., 1996) and in 15- to 20-dpf fish (Fig. 3; Table 1). In the neurocranium, we detected recombined tissues in the ethmoid plate (Fig. 3A, e), trabeculae (Fig. 3A, t), taenia marginalis anterior (Fig. 3B, tma) and posterior (Fig. 3B, tmp), epiphyseal bar (Fig. 3B, eb) and in the otic capsule (Fig. 3C), whereas the basilar plate (parachordalia) and the anterior basicranial commissure were devoid of labeled cells. In the viscerocranium, we found a NC contribution to all its components (Fig. 3D,E).

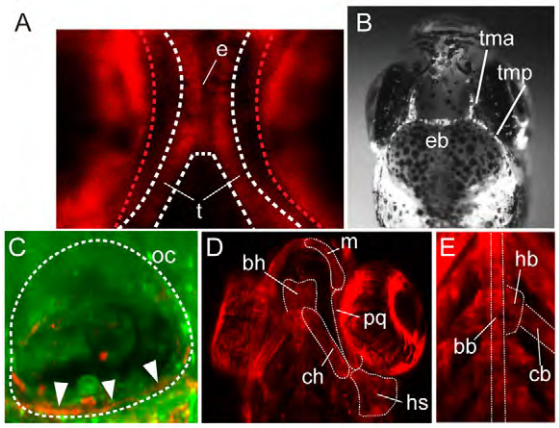

Fig. 3. NC-derived elements in the developing chondrocranium and viscerocranium. (**A**) Confocal section of recombined tissue in the ethmoid plate (e) and the trabeculae (t) of a 5-dpf *Tg(sox10:ER^{T2}-Cre;ubi:switch)* larva. The red dashed lines highlight the autofluorescence of the eyes. (**B**) Epifluorescent image of labeled elements of the dorsal neurocranium in 15-dpf *Tg(sox10:ER^{T2}-Cre;β-actin:switch)* fish: taenia marginalis anterior (tma), taenia marginalis posterior (tmp) and epiphyseal bar (eb). (C-E) MIP of confocal stacks. (**C**) Recombined cells in the forming ventral cartilage of the otic capsule (oc, arrowheads) in 5-dpf *Tg(sox10:ER^{T2}-Cre;ubi:switch)* larvae. (**D**) Labeled viscerocranial elements in the mandibular region [Meckel's cartilage (m), palatoquadrate (pq)] and in the hyod region [hyosymplectic (hs), ceratohyal (ch), basihyal (bh)] of 5-dpf *Tg(sox10:ER^{T2}-Cre;ubi:switch)* larvae. (**E**) Labeled basibranchial (bb), hypobranchial (hb) and ceratobranchial (cb) elements of 5-dpf *Tg(sox10:ER^{T2}-Cre;ubi:switch)* larvae.

In the head of metamorphic and adult fish we identified, by *in vivo* confocal imaging, neurocranial, viscerocranial and dermatocranial skeletal elements (Fig. 4; supplementary material Fig. S2). We decided to focus our attention on those structures that are still debated in the literature among different vertebrate taxa. Identifying their embryonic origin in zebrafish will be of great importance in deciphering key steps of vertebrate evolution.

First, we looked at the otic capsule and at the viscerocranium to confirm at later stages what we found in the larvae. A NC origin for the otic capsule cartilage has been shown previously in *Xenopus*, chicken and mice (Gross and Hanken, 2008b; Le Lièvre, 1978; Noden, 1983; Cubbage and Mabee, 1996; O'Gorman, 2005), whereas extirpation/vital dye labeling experiments did not demonstrate a NC contribution to this structure in lamprey, medaka or toads (Langille and Hall, 1988a; Langille and Hall, 1988b; Olsson and Hanken, 1996). Notably, in the neurocranium of juvenile zebrafish, we detected labeled chondroblasts and osteoblasts in the otic capsule and in the structure that contributes to the formation of the inner ear (Fig. 4A-A″).

In the viscerocranium, Meckel's cartilage, along with other important viscerocranial elements, is labeled, as expected (Fig. 4B). Remarkably, we detected labeled cells in the basihyal and the basibranchial (Fig. 4B′), two cartilages that form the hyobranchial skeleton. Unlike in zebrafish, NC does not seem to contribute to these bones in lissamphibians (Olsson and Hanken, 1996).

In the dermatocranium, we show that NC contributes to the entire opercular series, consisting of the opercle, inter-, sub- and preopercle (Fig. 4C,D). The vault series of dermal bones forming the roof of the skull consists of paired frontals and parietals. Both NC and mesoderm are known to contribute to frontoparietal bones. Intriguingly, we find that in zebrafish the frontals are labeled only in the anterior center of ossification (Fig. 4E, arrowhead; Fig. 4F) and the parietals (n=100, using three different reporter lines) are devoid of recombined osteoblasts (Fig. 4E, outlined by the dashed frame). The extent of their contribution defines a NC/mesoderm boundary in the skull, for which empirical data are inconsistent across vertebrate taxa (Gross and Hanken, 2008a). Our data point to a NC/mesoderm boundary in the frontal bones, at the border between the anterior and the posterior ossification centers.

NC contributes to the barbels

Barbels are whisker-like tactile organs that protrude from the integument of the mouth region. The embryonic origin of the fibroblast-like cells that synthesize the extracellular rod matrix is unknown. As barbels have been recently used as a model for adult organ regeneration (LeClair and Topczewski, 2010), we sought to determine whether NC contributes to barbel development.

We detected labeled cells at the core of the maxillary barbels, surrounded by specialized epithelial cells (Fig. 4G). Specifically, we identified labeled nerve fibers (Fig. 4H, asterisks, red channel) in the region of the lymphatic (Fig. 4H, arrow, green channel) and blood vessels (Fig. 4H, arrowhead, green channel). Notably, we

Table 1. List of chondrocranial and viscerocranial elements that form the developing skull with detected/undetected contribution from the NC

Division	Region	Element	NC contribution
Neurocranium	Base	Parachordal (pc)	Not detected
		Anterior basicranial commissure (abc)	Not detected
		Trabecula (t)	Yes
		Ethmoidal plate (e)	Yes
	Orbito-temporal	Epiphyseal bar (eb)	Yes
		Taenia marginalis anterior (tma)	Yes
		Taenia marginalis posterior (tmp)	Yes
	Otic	Otic capsule (oc)	Yes
Viscerocranium	Mandibular	Meckel's cartilage (m)	Yes
		Palatoquadrate (pq)	Yes
	Hyoid	Basihyal (bh)	Yes
		Ceratohyal (ch)	Yes
		Hyosymplectic (hs)	Yes
	Branchial	Basibranchial (bb)	Yes
		Hypobranchial (hb)	Yes
		Ceratobranchial (cb)	Yes

Abbreviations as in Fig. 3.

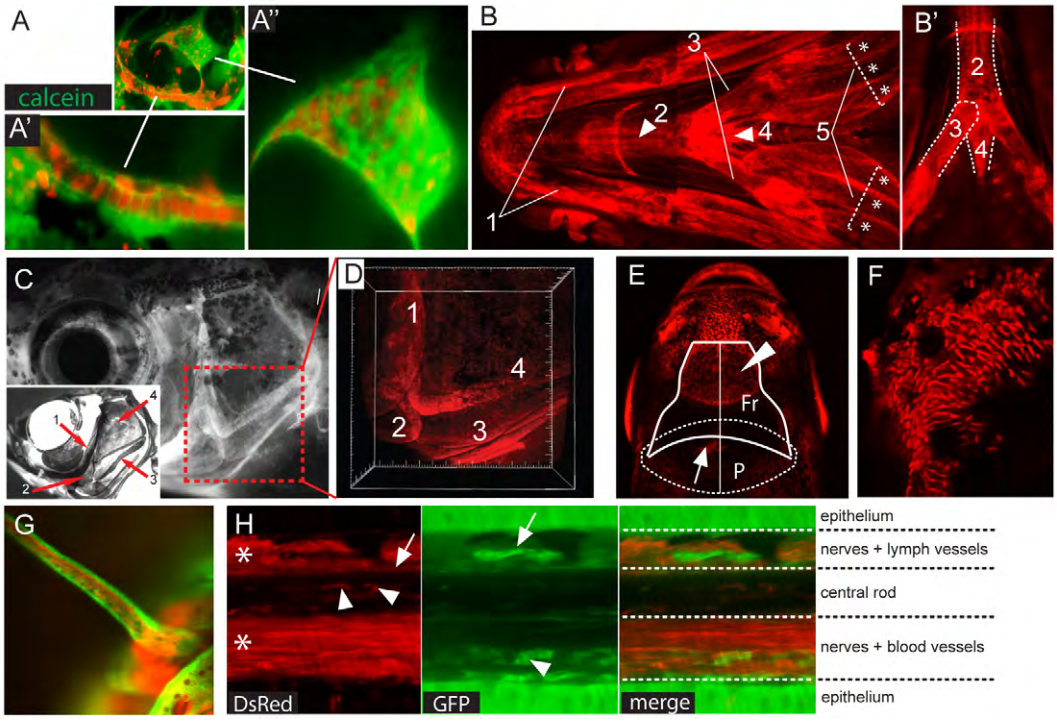

Fig. 4. Detection of contested cranial NC derivatives. (**A-A″**) MIP of confocal stacks showing labeled cartilaginous and bony elements in the otic capsule: chondroblasts and osteoblasts in the ventral cartilage (A′) and in the inner ear structures (A″). (**B**) MIP of confocal stacks (ventral view) showing labeled viscerocranial structures: (1) Meckel's cartilage (paired), (2) the basihyal (unpaired), (3) the ceratohyal (paired), (4) the basibranchial (unpaired) and (5) the branchiostegal rays (paired), with individual rays marked with an asterisk. (**B′**) Confocal section from B showing labeled (2) basihyal (unpaired), (3) ceratohyal (paired) and (4) basibranchial (unpaired) elements. (**C**,**D**) Epifluorescent image of mCherry^{+} osteoblasts forming the opercular series in *Tg(sox10:ER^{T2}-Cre;ubi:switch)* adult fish (C) and Alizarin Red-stained skull (lateral view) in a 3-month-old zebrafish showing the four bones forming the opercular series: (1) preopercle, (2) interopercle, (3) subopercle and (4) opercle (inset). (D) 3D view of confocal stacks (boxed region in C), which shows positive cells in all the bones composing the opercular series. (**E**) Frontal (Fr) and parietal (P) bones. Epifluorescence image showing recombined osteoblasts in the rostral part of the frontals (arrowhead), whereas the parietals are devoid of labeled osteoblasts (arrow indicates a pigment cell clone). (**F**) MIP of confocal stacks showing labeled osteoblasts in the anterior region of the frontals. (**G**) MIP of confocal stacks of a maxillary barbel in induced adult fish showing recombined tissues in the core of the tactile organ. (**H**) Confocal section showing, in the red channel, labeled nerves (asterisks), fibroblast-like cells in the rod matrix (arrowheads) and flattened cells along the dorsal aspect of the rod (arrow). In the green channel, a non-switched lymphatic vessel (arrow) and blood vessel (arrowhead) are indicated. In the merge panel, the different layers composing the barbels are shown.

found labeled fibroblast-like cells embedded in the matrix of the central rod (Fig. 4H, arrowheads, red channel) and labeled flattened cells along the dorsal aspect of the rod (Fig. 4H, arrow, red channel). Interestingly, similar mesenchymal, fibroblast-like cells have been proposed to play a crucial role in blastema formation during fin regeneration (Knopf et al., 2011).

Pillar cells are NC derived

Finally, we focused on the gill organ and observed labeled gill filaments, including primary and secondary lamellae (Fig. 5A,B). In the primary lamellae, smooth muscle cells of the blood vessel tunica media are labeled (Fig. 5C, arrows) and are located in close contact with the endothelium, which is labeled by the *flk:GFP* transgene (Lawson and Weinstein, 2002) (Fig. 5C′). In the secondary lamellae, we found labeled pillar cells (Fig. 5D,E). Pillar cells are highly specialized, with autoregulatory contractile properties that offer mechanical support to the respiratory epithelium (Fig. 5D, green), and enable an adaptation of the lamellar surface to the oxygen content of water (Bettex-Galland and Hughes, 1973; Hughes and Morgan, 1973). Pillar cells are arranged in parallel columns and, with their cytoplasmic processes (Fig. 5D, arrowhead) supporting the respiratory epithelium (Fig. 5D, green), form lumina (Fig. 5E, arrowheads) that give rise to capillary networks through which blood perfuses and gas exchange occurs (Fig. 5F) (Hughes and Morgan, 1973).

In our experimental set-up, the definition of NC origin rests entirely on the specificity of the *sox10* promoter. Although we did identify most of the previously known NC derivatives in the floxed clones, the discovery of new structures requires independent confirmation. We therefore induced recombination with an alternative NC promoter from the *crestin* locus (Luo et al., 2001) (Y.-Y. Chen, PhD thesis, Eberhard Karls Universität Tübingen, 2011) by injecting *UAS:Cre* DNA into *Tg(crestin:gal4-UAS:GFP;β-actin:switch)* embryos at the 1-cell stage. We detected, among previously identified NC derivatives (data not shown), labeled barbels (supplementary material Fig. S3), gill pillar cells and smooth muscles (Fig. 5G). Moreover, we identified these structures using a non-inducible *sox10:Cre* line with a longer (7.2 kb) promoter fragment and a different genomic insertion site (Rodrigues et al., 2012) (data not shown).

DISCUSSION

The appearance of NC was fundamental to subsequent vertebrate evolutionary history, tremendously accelerating the emergence

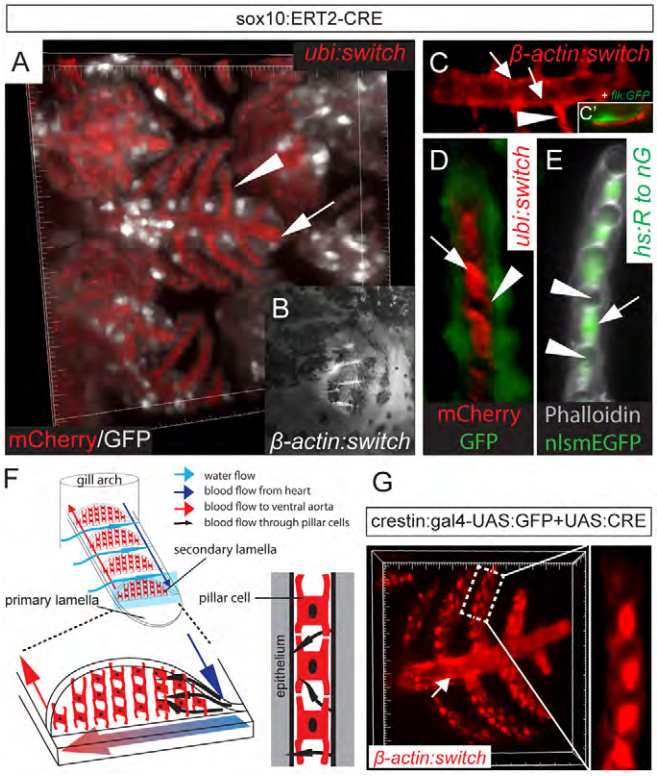

Fig. 5. NC origin of gill pillar cells. (A-E) Recombined cells in the primary and secondary lamellae of the gills. (**A**) 3D view of confocal stacks showing the gill lamellae in an induced *Tg(sox10:ER^{T2}-Cre;ubi:switch)* adult fish: non-NC-derived tissues are in gray (GFP), whereas NC-derived tissues in the primary (arrow) and in the secondary (arrowhead) lamellae are in red (mCherry). (**B**) Epifluorescence image of DsRed^{+} cells in the primary and secondary lamellae in an induced *Tg(sox10:ER^{T2}-Cre;β-actin:switch)* adult fish. (**C**) Confocal section of labeled smooth muscles of the blood vessel tunica media in the primary lamellae (arrows) and pillar cell in contact with the smooth muscle layer (arrowhead). (**C′**) flk:GFP^{+} endothelium in the gills surrounded by NC-derived smooth muscles. (**D**) Confocal section of a secondary lamellae showing recombined mCherry^{+} pillar cells surrounded by non-recombined GFP^{+} epithelial cells in an induced *Tg(sox10:ER^{T2}-Cre;ubi:switch)* adult fish. The arrow indicates the pillar cell body, whereas the arrowhead marks a cytoplasmic process connecting two neighboring pillar cells. (**E**) MIP of confocal stacks showing a phalloidin-stained (gray) secondary lamella with the GFP^{+} pillar cell nuclei of an induced *hs:R to nG* adult fish. The pillar cell nuclei (arrow) are located between adjacent lumina (arrowheads). (**F**) Schematic of gill lamellae and pillar cells demonstrating the flow of blood through the organ. (**G**) MIP of confocal stacks of recombined lamellae using the *crestin* promoter, showing labeled smooth muscles (arrow) and pillar cells (inset).

of a predatory lifestyle and the exploitation of unexplored ecological niches. Although NC contribution to multiple cell types is well documented in different model organisms (Gross and Hanken, 2008a), the lack of a comprehensive analysis of NC-derived adult structures in actinopterygians leaves a gap in our understanding of important evolutionary transitions. Key innovations that endowed vertebrates with predatory capacity were the acquisition of muscular ventilation coupled with respiratory surface expansion, the emergence of a skull vault and a dorsoventrally articulated jaw. We have developed and employed a genetic long-term labeling method to uncover a potential NC origin of evolutionarily important cell types and tissues of previously unrecognized or debated origin in zebrafish, a model teleost. In particular, in the present study we focused on the gill respiratory system and showed that, by giving rise to gill pillar cells, NC might have expedited respiratory surface expansion and muscular ventilation.

NC-driven expansion of the respiratory surface at the protochordate-vertebrate transition

At the protochordate-vertebrate transition, the acquisition of a predatory lifestyle was facilitated by a massive expansion of the respiratory surface in the gills and the switch from ciliary to muscular ventilation (Northcutt and Gans, 1983). Recent paleontological analysis of cristozoan fossils such as *Haikouella lanceolata* and *Yunnanozoon lividum* suggests a precraniate history of ‘crest animals’. These fossils are characterized by paired gill rays and jointed, widely spaced branchial arches, but do not possess a skull (Chen, 2008; Chen et al., 1999; Holland and Chen, 2001; Mallatt and Chen, 2003). Although many structures directly involved in prey capture have been shown to derive from NC, the embryonic origin of the new, expanded respiratory organ, which according to the recent paleontological interpretation seems to predate the appearance of the skull, has not been investigated. Our demonstration of a NC origin for gill pillar cells reinforces the importance of this embryonic tissue in the evolution of respiratory systems and, possibly, in the radiation of precraniate crest animals at the protochordate-vertebrate transition.

Pillar cells are found in the gills of hagfishes (Mallatt and Paulsen, 1986; Elger, 1987), lampreys (Youson and Freeman, 1976), chondrichthyans and osteognathostomes (Evans et al., 2005). However, cephalochordates lack specialized gill cells that increase the respiratory surface area. Instead, this group has rather simple collagen bars located in the pharynx atrium, and gas exchange occurs through ciliated epithelial cells (Welsch, 1975; Baskin and Detmers, 1976). Thus, pillar cells are a craniate synapomorphy and, as they provide the structural basis for the new expanded gill organ, represent a key innovation in vertebrate evolution. Pillar cells form small channels to conduct blood through the gills and possess the ability to expand or contract their cytoplasmic processes to control blood flow (Bettex-Galland and Hughes, 1973). This contraction/expansion activity also regulates the distance between neighboring secondary lamellae, thereby modulating water flow through the gills. The development of this atypical vertebrate-specific cell type is still poorly understood. Observations of cellular microanatomy and tissue ontogeny (Datta Munshi and Singh, 1968), supported by the expression of smooth muscle myosin (Smith and Chamley-Campbell, 1981), suggest a derivation of pillar cells from the smooth muscles forming the blood vessels of the primary lamellae. Cephalic NC is known to give rise to avian and mammalian smooth muscle cells of the blood vessels of the face and forebrain but not to the endothelium (Etchevers et al., 2001; Le Lièvre and Le Douarin, 1975; Yoshida et al., 2008). Our finding that, in addition to the smooth muscles of the pharyngeal arches, those forming the primary lamellae also have a NC origin supports the hypothesis that pillar cells evolved from this tissue rather than from endothelial cells, as originally proposed (Bietrix, 1895).

NC contribution to cranial skeletal elements and barbels in zebrafish

The contribution of cranial NC to the frontal and parietal bones is contentious and studies using different model systems and labeling techniques have led to inconsistent results (Couly et al., 1993;

Noden and Trainor, 2005; Gross and Hanken, 2008a). For example, fate mapping in *Xenopus* using fluorescent dextran labeling suggested that cranial NC contributes to the entire length of the frontoparietal bones (Gross and Hanken, 2005), whereas studies in mouse using *Wnt1-Cre*-mediated genetic labeling suggested that NC does not contribute to the parietal bones (Jiang et al., 2002). Moreover, analysis of quail-chick chimeras has led to conflicting conclusions regarding a NC contribution to these dermatocranial elements in the avian skull, defining the NC-mesoderm boundary at the border between the anterior and posterior regions of the frontals (Noden, 1978; Evans and Noden, 2006) or extending NC contributions to both frontal and parietal bones (Couly et al., 1993).

The frontal and parietal bones of the zebrafish are anatomically similar to their mammalian counterparts and start to ossify at 3-4 weeks postfertilization (Cubbage and Mabee, 1996; Quarto and Longaker, 2005). We find that NC contributes to the anterior but not to the posterior ossification center of the frontals. Further, we find no contribution to the parietals, allowing us to suggest that the NC/mesoderm boundary in zebrafish lies in the frontal bones, between the anterior and the posterior ossification center, as has been shown in chicken (Noden, 1978; Evans and Noden, 2006) and mice (Jiang et al., 2002). Differences in the location of the NC/mesoderm boundary could also be attributed to species-specific factors, although we cannot rule out a possible contribution of experimental methodology to conflicting conclusions.

The embryonic origin of the otic capsule is debated. These paired bones accommodating the inner ear are considered to be a novelty of craniates and are absent in early crest animals (Chen, 2008; Gross and Hanken, 2008a; Mallatt and Chen, 2003). Studies in birds and mammals have shown a NC contribution to the otic capsule (Le Lièvre, 1978; O'Gorman, 2005; Noden, 1983). Previous studies using NC extirpation/vital dye labeling did not find a NC contribution to the otic capsules in lamprey (Langille and Hall, 1988b), medaka (Langille and Hall, 1988a) and oriental fire-bellied toad (Olsson and Hanken, 1996), although the otic capsules in *Xenopus* were shown to receive a contribution from the cranial NC (Gross and Hanken, 2008b). These studies have led to the view that NC contribution to the otic capsule must predate the divergence of the mammalian and avian lineages (O'Gorman, 2005; Gross and Hanken, 2008a). We show that NC contributes to the otic capsule in zebrafish and could thus be a trait shared among vertebrates. In this regard, it is interesting to note that mutants with NC defects often have ear phenotypes in zebrafish (Kelsh et al., 1996; Whitfield et al., 1996).

Elegant fossil and molecular genetic analyses suggest that gnathostome jaw evolution occurred in a stepwise fashion, facilitated by skull reorganization and altered epithelial-mesenchymal interactions among pre-existing molecular programs (Gai et al., 2011; Shigetani et al., 2002). We find that, as in other vertebrates, the complete lower jaw is NC derived. Contrary to observations in amphibians (Olsson and Hanken, 1996), the zebrafish hypobranchial skeleton is also NC derived.

The opercular flap, which consists of multiple flat dermal bones, is also NC derived, as shown in the present study. The evolution of the opercular series has facilitated a novel mechanism for the depression of the mandible (Lauder, 1980a; Lauder, 1980b; Lauder, 1982), allowing an improvement in suction feeding through better control over fluid movement (Lauder, 1980a). The NC origin of the opercular series, as conclusively shown using our long-term labeling approach, was previously assumed on the basis of its dermal bone composition and the expression of specific transgenes (Kimmel et al., 2010). Recent findings demonstrating the presence of an embryonic operculum in amniotes have rekindled interest in this structure, which was presumed to have been lost completely with the evolution of tetrapods and the emergence of a terrestrial lifestyle (Richardson et al., 2012).

We also find a NC contribution to zebrafish barbels. Barbels are tentacle-like chemosensory structures that arose independently many times during actinopterygian evolution (LeClair and Topczewski, 2010). Poor homology in terms of embryonic development and cellular composition across different vertebrate taxa complicates phylogenetic comparisons and makes it difficult to trace the evolutionary history of these sensory structures (Fox, 1999). In the barbels of recombined fish we detected fibroblast-like cells in the matrix of the rod and flattened cells along its dorsal aspect. These two cell types are likely to be involved in the production of the connective tissue of the supporting central rod. Barbels are an attractive model for understanding tissue regeneration in adult organs (LeClair and Topczewski, 2010). That central components of these structures have a NC origin raises the intriguing possibility of studying the potential role of NC-derived adult tissues in organ repair.

sox10:ER^{T2}-Cre as a tool to understand the evolution of developmental mechanisms underlying emergence of the vertebrate body plan

Very little is known about the cellular and molecular events underlying NC-driven diversification of the vertebrate body plan. This is due, in part, to a dearth of tools to allow consistent and long-term labeling of NC derivatives. Inducible *sox10:ER^{T2}-Cre* recombination allows NC long-term labeling in a spatiotemporal manner: the spatial domain of Cre-mediated recombination is restricted by the *sox10* promoter and the temporal domain is under tamoxifen control. In the future, the *sox10:ER^{T2}-Cre* line will also enable the genetic manipulation of NC and its derivatives. For example, taking advantage of the new FlipTrap and FlEx technologies (Trinh et al., 2011; Ni et al., 2012), it will be possible to specifically manipulate particular genes in cell lineages that fall into the spatiotemporal domain of the *sox10:ER^{T2}-Cre* transgene. This will greatly improve our understanding of how these populations of migratory and proliferative cells give rise to diverse cell types and organs in the vertebrate body.

In summary, using an inducible Cre/loxP system for genetic lineage tracing, we demonstrate a NC contribution to various structures in metamorphic and adult zebrafish, an important model teleost. In particular, our analysis reveals a direct involvement of NC in the development of gill pillar cells, an atypical cell type found in vertebrates and hagfishes. A switch from ciliary ventilation to respiratory muscular ventilation with gills was an early event during the evolutionary history of modern vertebrates, followed by skull reorganization and the emergence of a jaw. A role for the NC in remodeling the respiratory system of early crest animals is underappreciated, in part owing to the lack of such analyses in non-tetrapod vertebrates. Respiratory systems underwent a profound transformation and pillar cells were lost along the tetrapod lineage. We propose that the evolution of the gills, with their highly expanded respiratory surface, was driven by the NC, and thus confirm the fundamental role played by this embryonic tissue in vertebrate radiation.

Acknowledgements

We thank F. Argenton, C. Baker, R. Kelsh and all our colleagues for insightful discussion and helpful comments on the manuscript; F. S. Rodrigues (R. Kelsh laboratory) for sharing unpublished data; and C. Dooley for valuable support in the early phases of this work.

Funding
This work was funded by the Max-Planck Society for the Advancement of Science and the European Molecular Biology Organization to A.P.S.

Competing interests statement
The authors declare no competing financial interests.

Supplementary material
Supplementary material available online at
http://dev.biologists.org/lookup/suppl/doi:10.1242/dev.091066/-/DC1

References
Abitua, P. B., Wagner, E., Navarrete, I. A. and Levine, M. (2012). Identification of a rudimentary neural crest in a non-vertebrate chordate. *Nature* **492**, 104-107.
Baskin, D. G. and Detmers, P. A. (1976). Electron microscopic study on the gill bars of amphioxus (Branchiostoma californiense) with special reference to neurociliary control. *Cell Tissue Res.* **166**, 167-178.
Bertrand, J. Y., Chi, N. C., Santoso, B., Teng, S., Stainier, D. Y. and Traver, D. (2010). Haematopoietic stem cells derive directly from aortic endothelium during development. *Nature* **464**, 108-111.
Bettex-Galland, M. and Hughes, G. M. (1973). Contractile filamentous material in the pillar cells of fish gills. *J. Cell Sci.* **13**, 359-370.
Bietrix, E. (1895). Quelques considerations sur les notions de lacune et d'endothelium en anatomie generale, a propos du rescau vasculaire branchial des Poissons. *C. R. Somm. Seanc. Soc. Philomath.* **189**, 26-28.
Bronner-Fraser, M. and Fraser, S. E. (1988). Cell lineage analysis reveals multipotency of some avian neural crest cells. *Nature* **335**, 161-164.
Carney, T. J., Dutton, K. A., Greenhill, E., Delfino-Machín, M., Dufourcq, P., Blader, P. and Kelsh, R. N. (2006). A direct role for Sox10 in specification of neural crest-derived sensory neurons. *Development* **133**, 4619-4630.
Chai, Y., Jiang, X. B., Ito, Y., Bringas, P., Jr, Han, J., Rowitch, D. H., Soriano, P., McMahon, A. P. and Sucov, H. M. (2000). Fate of the mammalian cranial neural crest during tooth and mandibular morphogenesis. *Development* **127**, 1671-1679.
Chen, J. Y. (2008). Early crest animals and the insight they provide into the evolutionary origin of craniates. *Genesis* **46**, 623-639.
Chen, J. Y., Huang, D. Y. and Li, C. W. (1999). An early Cambrian craniate-like chordate. *Nature* **402**, 518-522.
Collazo, A., Bronner-Fraser, M. and Fraser, S. E. (1993). Vital dye labelling of Xenopus laevis trunk neural crest reveals multipotency and novel pathways of migration. *Development* **118**, 363-376.
Couly, G. F., Coltey, P. M. and Le Douarin, N. M. (1993). The triple origin of skull in higher vertebrates: a study in quail-chick chimeras. *Development* **117**, 409-429.
Cubbage, C. C. and Mabee, P. M. (1996). Development of the cranium and paired fins in the zebrafish Danio rerio (Ostariophysi, cyprinidae). *J. Morphol.* **229**, 121-160.
Datta Munshi, J. S. and Singh, B. N. (1968). On the micro-circulatory system of the gills of certain freshwater teleostean fishes. *J. Zool.* **154**, 365-376.
Dutton, K. A., Pauliny, A., Lopes, S. S., Elworthy, S., Carney, T. J., Rauch, J., Geisler, R., Haffter, P. and Kelsh, R. N. (2001). Zebrafish colourless encodes sox10 and specifies non-ectomesenchymal neural crest fates. *Development* **128**, 4113-4125.
Elger, M. (1987). The branchial circulation and the gill epithelia in the Atlantic hagfish, Myxine glutinosa L. *Anat. Embryol. (Berl.)* **175**, 489-504.
Etchevers, H. C., Couly, G., Vincent, C. and Le Douarin, N. M. (1999). Anterior cephalic neural crest is required for forebrain viability. *Development* **126**, 3533-3543.
Etchevers, H. C., Vincent, C., Le Douarin, N. M. and Couly, G. F. (2001). The cephalic neural crest provides pericytes and smooth muscle cells to all blood vessels of the face and forebrain. *Development* **128**, 1059-1068.
Evans, D. J. and Noden, D. M. (2006). Spatial relations between avian craniofacial neural crest and paraxial mesoderm cells. *Dev. Dyn.* **235**, 1310-1325.
Evans, D. H., Piermarini, P. M. and Choe, K. P. (2005). The multifunctional fish gill: dominant site of gas exchange, osmoregulation, acid-base regulation, and excretion of nitrogenous waste. *Physiol. Rev.* **85**, 97-177.
Fox, H. (1999). Barbels and barbel-like tentacular structures in sub-mammalian vertebrates: a review. *Hydrobiologia* **403**, 153-193.
Gai, Z., Donoghue, P. C., Zhu, M., Janvier, P. and Stampanoni, M. (2011). Fossil jawless fish from China foreshadows early jawed vertebrate anatomy. *Nature* **476**, 324-327.
Gans, C. and Northcutt, R. G. (1983). Neural crest and the origin of vertebrates: a new head. *Science* **220**, 268-273.
Gross, J. B. and Hanken, J. (2005). Cranial neural crest contributes to the bony skull vault in adult Xenopus laevis: insights from cell labeling studies. *J. Exp. Zool.* **304B**, 169-176.
Gross, J. B. and Hanken, J. (2008a). Review of fate-mapping studies of osteogenic cranial neural crest in vertebrates. *Dev. Biol.* **317**, 389-400.
Gross, J. B. and Hanken, J. (2008b). Segmentation of the vertebrate skull: neural-crest derivation of adult cartilages in the clawed frog, Xenopus laevis. *Integr. Comp. Biol.* **48**, 681-696.
Hans, S., Kaslin, J., Freudenreich, D. and Brand, M. (2009). Temporally-controlled site-specific recombination in zebrafish. *PLoS ONE* **4**, e4640.
Holland, N. D. and Chen, J. (2001). Origin and early evolution of the vertebrates: new insights from advances in molecular biology, anatomy, and palaeontology. *BioEssays* **23**, 142-151.
Hörstadius, S. (1950). *The Neural Crest: Its Properties and Derivatives in the Light of Experimental Research*. London: Oxford University Press.
Hughes, G. M. and Morgan, M. (1973). The structure of fish gills in relation to their respiratory function. *Biol. Rev. Camb. Philos. Soc.* **48**, 419-475.
Jiang, X., Iseki, S., Maxson, R. E., Sucov, H. M. and Morriss-Kay, G. M. (2002). Tissue origins and interactions in the mammalian skull vault. *Dev. Biol.* **241**, 106-116.
Kelsh, R. N., Brand, M., Jiang, Y. J., Heisenberg, C. P., Lin, S., Haffter, P., Odenthal, J., Mullins, M. C., van Eeden, F. J. M., Furutani-Seiki, M. et al. (1996). Zebrafish pigmentation mutations and the processes of neural crest development. *Development* **123**, 369-389.
Kimmel, C. B., DeLaurier, A., Ullmann, B., Dowd, J. and McFadden, M. (2010). Modes of developmental outgrowth and shaping of a craniofacial bone in zebrafish. *PLoS ONE* **5**, e9475.
Knopf, F., Hammond, C., Chekuru, A., Kurth, T., Hans, S., Weber, C. W., Mahatma, G., Fisher, S., Brand, M., Schulte-Merker, S. et al. (2011). Bone regenerates via dedifferentiation of osteoblasts in the zebrafish fin. *Dev. Cell* **20**, 713-724.
Kwan, K. M., Fujimoto, E., Grabher, C., Mangum, B. D., Hardy, M. E., Campbell, D. S., Parant, J. M., Yost, H. J., Kanki, J. P. and Chien, C. B. (2007). The Tol2kit: a multisite gateway-based construction kit for Tol2 transposon transgenesis constructs. *Dev. Dyn.* **236**, 3088-3099.
Landacre, F. L. (1921). The fate of the NC in the head of the Urodeles. *J. Comp. Neurol.* **33**, 1-43.
Langille, R. M. and Hall, B. K. (1988a). Role of the neural crest in development of the cartilaginous cranial and visceral skeleton of the medaka, Oryzias latipes (Teleostei). *Anat. Embryol. (Berl.)* **177**, 297-305.
Langille, R. M. and Hall, B. K. (1988b). Role of the neural crest in development of the trabeculae and branchial arches in embryonic sea lamprey, Petromyzon-Marinus (L). *Development* **102**, 301-310.
Lauder, G. V. (1980a). Evolution of the feeding mechanism in primitive actinopterygian fishes – a functional anatomical analysis of Polypterus, Lepisosteus, and Amia. *J. Morphol.* **163**, 283-317.
Lauder, G. V. (1980b). On the evolution of the jaw adductor musculature in primitive gnathostome fishes. *Breviora* **460**, 1-10.
Lauder, G. V. (1982). Patterns of evolution in the feeding mechanism of actinopterygian fishes. *Am. Zool.* **22**, 275-285.
Lawson, N. D. and Weinstein, B. M. (2002). In vivo imaging of embryonic vascular development using transgenic zebrafish. *Dev. Biol.* **248**, 307-318.
Le Douarin, N. M. (1986). Cell line segregation during peripheral nervous system ontogeny. *Science* **231**, 1515-1522.
Le Douarin, N. M. and Dupin, E. (2012). The neural crest in vertebrate evolution. *Curr. Opin. Genet. Dev.* **22**, 381-389.
Le Douarin, N. M. and Kalcheim, C. (1999). *The Neural Crest*. Cambridge: Cambridge University Press.
Le Lièvre, C. S. (1978). Participation of neural crest-derived cells in the genesis of the skull in birds. *J. Embryol. Exp. Morphol.* **47**, 17-37.
Le Lièvre, C. S. and Le Douarin, N. M. (1975). Mesenchymal derivatives of the neural crest: analysis of chimaeric quail and chick embryos. *J. Embryol. Exp. Morphol.* **34**, 125-154.
LeClair, E. E. and Topczewski, J. (2010). Development and regeneration of the zebrafish maxillary barbel: a novel study system for vertebrate tissue growth and repair. *PLoS ONE* **5**, e8737.
Li, Y. X., Zdanowicz, M., Young, L., Kumiski, D., Leatherbury, L. and Kirby, M. L. (2003). Cardiac neural crest in zebrafish embryos contributes to myocardial cell lineage and early heart function. *Dev. Dyn.* **226**, 540-550.
Luo, R., An, M., Arduini, B. L. and Henion, P. D. (2001). Specific pan-neural crest expression of zebrafish Crestin throughout embryonic development. *Dev. Dyn.* **220**, 169-174.
Mallatt, J. and Paulsen, C. (1986). Gill ultrastructure of the Pacific hagfish Eptatretus stouti. *Am. J. Anat.* **177**, 243-269.
Mallatt, J. and Chen, J. Y. (2003). Fossil sister group of craniates: predicted and found. *J. Morphol.* **258**, 1-31.
Metzger, D., Clifford, J., Chiba, H. and Chambon, P. (1995). Conditional site-specific recombination in mammalian cells using a ligand-dependent chimeric Cre recombinase. *Proc. Natl. Acad. Sci. USA* **92**, 6991-6995.
Mosimann, C., Kaufman, C. K., Li, P., Pugach, E. K., Tamplin, O. J. and Zon, L. I. (2011). Ubiquitous transgene expression and Cre-based recombination driven by the ubiquitin promoter in zebrafish. *Development* **138**, 169-177.

Ni, T. T., Lu, J., Zhu, M., Maddison, L. A., Boyd, K. L., Huskey, L., Ju, B., Hesselson, D., Zhong, T. P., Page-McCaw, P. S. et al. (2012). Conditional control of gene function by an invertible gene trap in zebrafish. *Proc. Natl. Acad. Sci. USA* **109**, 15389-15394.
Noden, D. M. (1978). The control of avian cephalic neural crest cytodifferentiation. I. Skeletal and connective tissues. *Dev. Biol.* **67**, 296-312.
Noden, D. M. (1983). The role of the neural crest in patterning of avian cranial skeletal, connective, and muscle tissues. *Dev. Biol.* **96**, 144-165.
Noden, D. M. and Trainor, P. A. (2005). Relations and interactions between cranial mesoderm and neural crest populations. *J. Anat.* **207**, 575-601.
Northcutt, R. G. (2005). The new head hypothesis revisited. *J. Exp. Zool.* **304B**, 274-297.
Northcutt, R. G. and Gans, C. (1983). The genesis of neural crest and epidermal placodes: a reinterpretation of vertebrate origins. *Q. Rev. Biol.* **58**, 1-28.
O'Gorman, S. (2005). Second branchial arch lineages of the middle ear of wild-type and Hoxa2 mutant mice. *Dev. Dyn.* **234**, 124-131.
Olsson, L. and Hanken, J. (1996). Cranial neural-crest migration and chondrogenic fate in the oriental fire-bellied toad Bombina orientalis: Defining the ancestral pattern of head development in anuran amphibians. *J. Morphol.* **229**, 105-120.
Piotrowski, T., Schilling, T. F., Brand, M., Jiang, Y. J., Heisenberg, C. P., Beuchle, D., Grandel, H., van Eeden, F. J., Furutani-Seiki, M., Granato, M. et al. (1996). Jaw and branchial arch mutants in zebrafish II: anterior arches and cartilage differentiation. *Development* **123**, 345-356.
Quarto, N. and Longaker, M. T. (2005). The zebrafish (Danio rerio): a model system for cranial suture patterning. *Cells Tissues Organs* **181**, 109-118.
Richardson, J., Shono, T., Okabe, M. and Graham, A. (2012). The presence of an embryonic opercular flap in amniotes. *Proc. Biol. Sci.* **279**, 224-229.
Rodrigues, F. S., Doughton, G., Yang, B. and Kelsh, R. N. (2012). A novel transgenic line using the Cre-lox system to allow permanent lineage-labeling of the zebrafish neural crest. *Genesis* **50**, 750-757.
Sato, M. and Yost, H. J. (2003). Cardiac neural crest contributes to cardiomyogenesis in zebrafish. *Dev. Biol.* **257**, 127-139.
Schilling, T. F. and Kimmel, C. B. (1994). Segment and cell type lineage restrictions during pharyngeal arch development in the zebrafish embryo. *Development* **120**, 483-494.
Schilling, T. F., Piotrowski, T., Grandel, H., Brand, M., Heisenberg, C. P, Jiang, Y. J., Beuchle, D., Hammerschmidt, M., Kane, D. A., Mullins, M. C. et al. (1996). Jaw and branchial arch mutants in zebrafish I: branchial arches. *Development* **123**, 329-344.
Shigetani, Y., Sugahara, F., Kawakami, Y., Murakami, Y., Hirano, S. and Kuratani, S. (2002). Heterotopic shift of epithelial-mesenchymal interactions in vertebrate jaw evolution. *Science* **296**, 1316-1319.
Simon, C., Lickert, H., Götz, M. and Dimou, L. (2012). Sox10-iCreERT2 : a mouse line to inducibly trace the neural crest and oligodendrocyte lineage. *Genesis* **50**, 506-515.
Smith, D. G. and Chamley-Campbell, J. (1981). Localization of smooth-muscle myosin in branchial pillar cells of snapper (Chrysophys auratus) by immunofluorescence histochemistry. *J. Exp. Zool.* **215**, 121-124.
Trinh, A., Hochgreb, T., Graham, M., Wu, D., Ruf-Zamojski, F., Jayasena, C. S., Saxena, A., Hawk, R., Gonzalez-Serricchio, A., Dixson, A. et al. (2011). A versatile gene trap to visualize and interrogate the function of the vertebrate proteome. *Genes Dev.* **25**, 2306-2320.
Wada, N., Javidan, Y., Nelson, S., Carney, T. J., Kelsh, R. N. and Schilling, T. F. (2005). Hedgehog signaling is required for cranial neural crest morphogenesis and chondrogenesis at the midline in the zebrafish skull. *Development* **132**, 3977-3988.
Welsch, U. (1975). The fine structure of the pharynx, cyrtopodocytes and digestive caecum of amphioxus (Branchiostoma lanceolatum). *Symp. Zool. Soc. Lond.* **36**, 17-41.
Whitfield, T. T., Granato, M., van Eeden, F. J. M., Schach, U., Brand, M., Furutani-Seiki, M., Haffter, P., Hammerschmidt, M., Heisenberg, C. P., Jiang, Y. J. et al. (1996). Mutations affecting development of the zebrafish inner ear and lateral line. *Development* **123**, 241-254.
Yoshida, T., Vivatbutsiri, P., Morriss-Kay, G., Saga, Y. and Iseki, S. (2008). Cell lineage in mammalian craniofacial mesenchyme. *Mech. Dev.* **125**, 797-808.
Youson, J. H. and Freeman, P. A. (1976). Morphology of the gills of larval and parasitic adult sea lamprey, Petromyzon marinus L. *J. Morphol.* **149**, 73-103.
Yu, J. K., Meulemans, D., McKeown, S. J. and Bronner-Fraser, M. (2008). Insights from the amphioxus genome on the origin of vertebrate neural crest. *Genome Res.* **18**, 1127-1132.

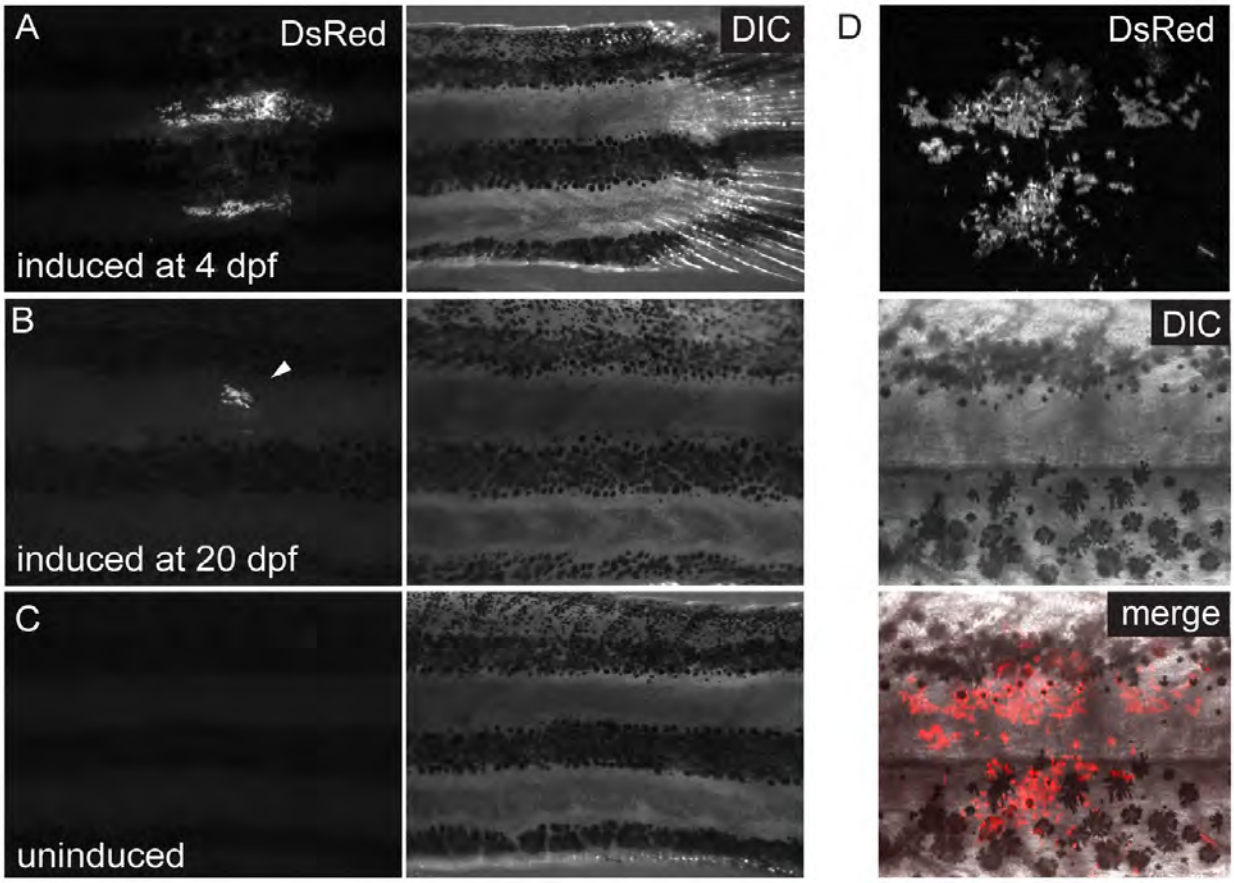

Fig. S1. Control of postembryonic Cre induction. (**A-C**) Epifluorescent acquisitions and brightfield images. (A) Pigment cell clones in adult fish induced at 4 dpf and (B) 20 dpf (arrowhead). (C) Trunk of uninduced adult fish devoid of clones. (**D**) MIP of confocal stacks showing labeled melanophores and iridophores on the adult fish flank.

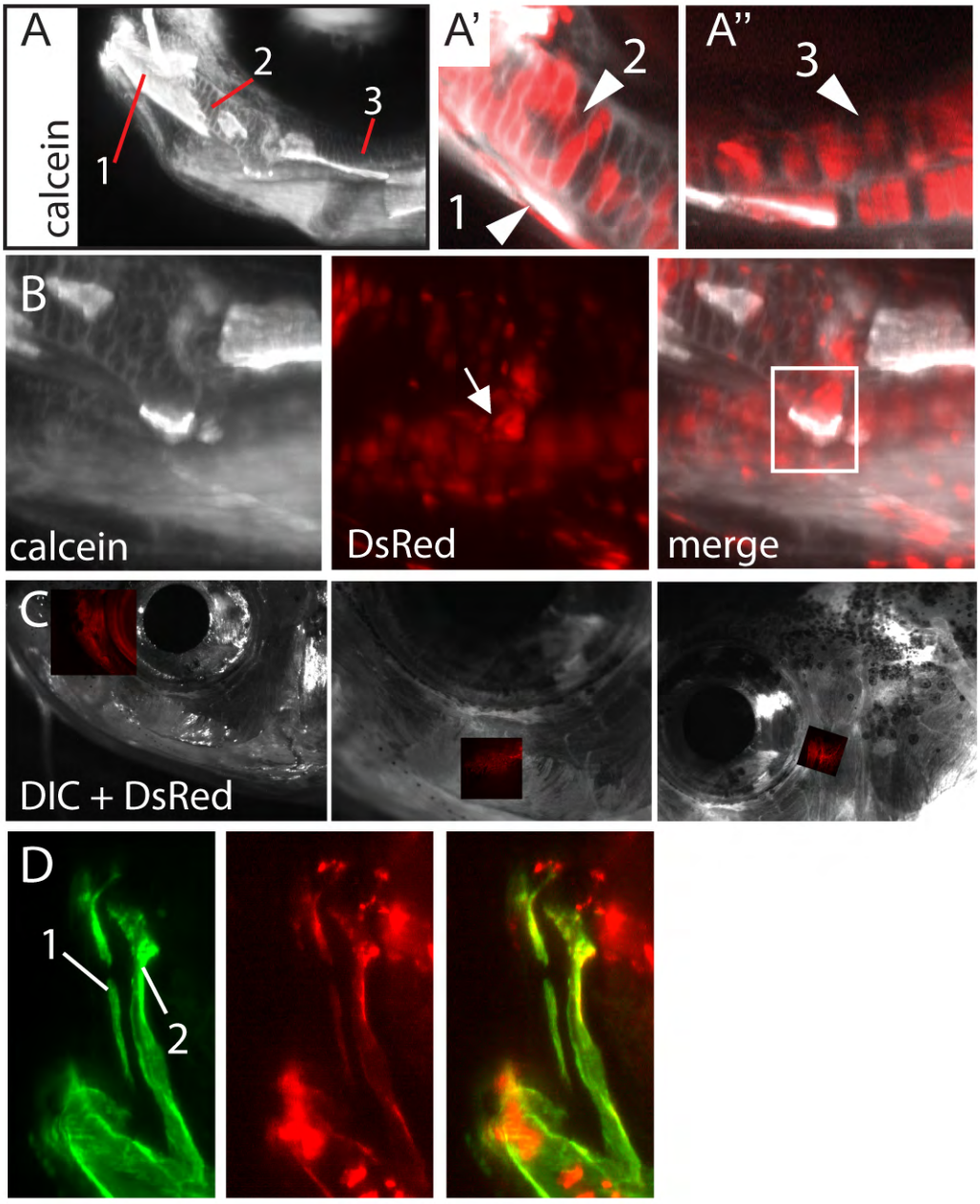

Fig. S2. Examples of NC-derived structures detectable *in vivo* in metamorphic and adult fish. (A-D) Induced *Tg(sox10:ER^{T2}-Cre;*β*-actin:switch)* metamorphic and adult fish stained with calcein. (**A-A′′′**) 20-dpf fish with labeled dentary (A′, 1), Meckel's cartilage (A′, 2) and palatoquadrate (A″, 3). (**B**) 20-dpf fish with labeled retroarticular bone (arrow). (**C**) Labeled circumorbital bones. (**D**) Labeled pre-maxilla (1) and maxilla (2).

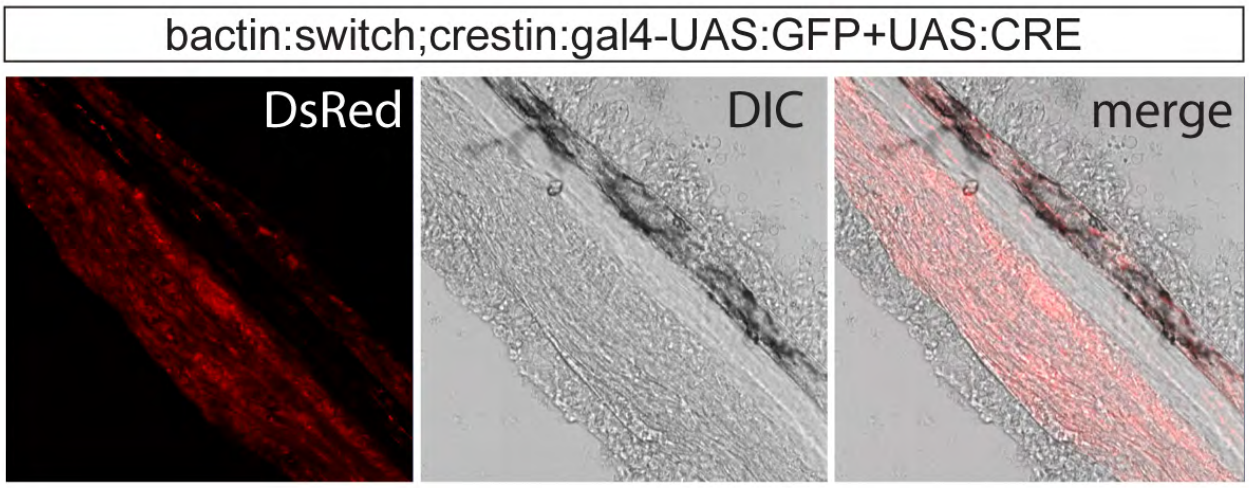

Fig. S3. Recombined tissues in barbels of adult *Tg(crestin:gal4-UAS:GFP;*β*-actin:switch)* fish injected at the 1-cell stage with *UAS:Cre* DNA.